



# The preparation and spontaneous imbibition of carbon-based nanofluid for enhanced oil recovery in tight reservoirs

Mingwei Zhao\*, Xuguang Song, Wenjiao Lv, Yining Wu, Caili Dai\*

Key Laboratory of Unconventional Oil & Gas Development, Ministry of Education, School of Petroleum Engineering, China University of Petroleum (East China), Qingdao, Shandong 266580, China  
Shandong Key Laboratory of Oilfield Chemistry, School of Petroleum Engineering, China University of Petroleum (East China), Qingdao 266580, China

## ARTICLE INFO

### Article history:

Received 16 April 2020

Received in revised form 4 June 2020

Accepted 8 June 2020

Available online 11 June 2020

### Keywords:

CNPs

Spontaneous imbibition

Tight reservoirs

Capillary force

## ABSTRACT

In this work, carbon-based nanofluid was prepared composed of hydrophilic carbon nanoparticles (CNPs) and Tween-80 to enhance oil recovery through spontaneous imbibition in tight reservoirs. The CNPs were characterized by transmission electron microscopy (TEM), dynamic light scattering (DLS), <sup>1</sup>HNMR, interfacial tension and wettability measurements. The particle size of CNPs was <10 nm and CNPs nanofluid showed excellent stability at high temperature and high salinity. CNPs nanofluid exhibited a stronger ability to reduce interfacial tension and change wettability than brine. The <sup>1</sup>HNMR imaging showed that CNPs had seeped into the core. The spontaneous imbibition tests showed that the spontaneous imbibition oil recovery of CNPs nanofluid can reach 24%, compared with 11% oil recovery of NaCl solution. CNPs nanofluid can efficiently enhance oil recovery, which was related to capillary force and structural disjoining pressure. CNPs nanofluid has great potential for enhancing oil recovery, especially in tight reservoirs.

© 2020 Published by Elsevier B.V.

## 1. Introduction

In recent years, unconventional oil resources [1–3] with great potential, especially tight reservoirs, have become an international hot spot of oil resources exploration and development. Due to the extremely low permeabilities, the development of tight reservoirs in unconventional oil resources is the most difficult [4–6]. The conventional water flooding in tight reservoirs often fails to achieve good effects. The oil recovery is lower than others due to low porosity and poor connectivity. It is usually necessary to reconstruct the reservoirs through fracturing technology to obtain the effective seepage channel [7,8]. Fracturing is an effective technology to improve formation conductivity by injecting excess fracturing fluids to open formation and supporting fractures by proppants [9]. After fracturing, water flooding is the main way to enhance oil recovery, which is generally ineffective to remove the oil from small pore throats.

Spontaneous imbibition is regarded as a very important oil recovery mechanism in tight reservoirs. Spontaneous imbibition is a process in which the wetting phase in porous media displaces the non-wetting phase under the action of capillary force [10–12]. Surfactant is a commonly used spontaneous imbibition agent, which can improve the wettability of core surface and reduce the interfacial tension between oil

and water [13–19]. The oil recovery of tight reservoirs can be improved by reducing the interfacial tension between oil and water, changing the wettability of rock and emulsifying dispersed oil droplets. Compared with water flooding, surfactant flooding has greater penetration depth and higher oil displacement efficiency. However, the presence of surfactant makes the produced oil form oil-in-water, water-in-oil or more complex emulsions. Demulsification of emulsion will greatly increase the production cost.

In recent years, nanomaterials, such as nanosilica (SiO<sub>2</sub>), nano-titanium dioxide (TiO<sub>2</sub>) and nano-aluminium oxide (Al<sub>2</sub>O<sub>3</sub>), have been studied and applied more and more in the oil and gas development field [20–22]. The nanomaterials have very small particle size and large specific surface area. Owing to virtue of the unique nano-effect, nanomaterials can enter into the porous medium and effectively adsorb on the interface to improve the interfacial properties. Laboratory tests showed that nanomaterials can improve the effects of core spontaneous imbibition tests and core displacement tests. Among all these nanomaterials, silica nanoparticles are the most widely studied. Onyekonwu and Ogolo [23] reported the performance of polysilicon nanoparticles for enhanced oil recovery by changing rock wettability and reducing interfacial tension. Ju et al. [24] verified that the hydrophilic nano-silica (LHP) can adsorb on the pore surface and change the surface wettability from hydrophobicity to hydrophilicity. Ponnappati [25] developed water dispersible SiO<sub>2</sub> – ethylene-oxide-based polymer nanohybrids. Hendraningrat et al. [26] proved that the displacement efficiency of functional silica nanoparticles was the highest in the neutral wetted core. Our group has done a lot of researches on silica nanofluids

\* Corresponding authors at: Key Laboratory of Unconventional Oil & Gas Development, Ministry of Education, School of Petroleum Engineering, China University of Petroleum (East China), Qingdao, Shandong 266580, China.

E-mail addresses: [zhaomingwei@upc.edu.cn](mailto:zhaomingwei@upc.edu.cn) (M. Zhao), [daic@upc.edu.cn](mailto:daic@upc.edu.cn) (C. Dai).

to enhance oil recovery. Zhao and Dai [27,28] presented that surfactant modified silica nanofluids can improve recovery in low permeability reservoirs by changing wettability. A surfactant-free carboxyl modified silica nanoparticles were prepared and used for EOR in tight sandstone cores [29]. Although there are a lot of researches on nanosilica, the silica nanofluids are not widely used in oil fields. One of the most important problems in the application of silica nanofluid is the stability. Silica nanofluid is not suitable for long time at high temperature and high salinity reservoirs. As a result, some scholars have begun to study carbon nanomaterials [30].

Due to the unique physical and chemical properties, carbon nanomaterials have attracted more and more attention in the field of oil and gas field development. The particle size of carbon nanoparticles is about 10 nm, they can enter the pores of porous media and play an important role on the pore surface and oil-water interface [31,32]. At present, there are also some researches on carbon nanoparticles in EOR. Soleimania [33] investigated the influence of carbon nanotubes based nanofluid on interfacial tension and oil recovery efficiency. Luo et al. [34] presented that low concentration nanofluid of graphene-based amphiphilic Janus nanosheets can achieve high oil recovery. Li [35] prepared a novel nanofluid based on fluorescent carbon nanoparticles for EOR. At present, the application of carbon nanoparticles is mainly focused on low permeability reservoirs, while the research on tight reservoirs has not been carried out. In this paper, we focus on the application of carbon nanoparticles to enhance oil recovery in tight reservoirs.

In this study, the hydrophilic carbon nanoparticles (CNPs) were prepared through electrolytic process. CNPs can be dispersed well in water by adding Tween-80. CNPs nanofluid has small particle size and strong stability at high salinity and high temperature. CNPs nanofluid has excellent ability for changing the wettability from oil-wet to natural-wet. The oil displacement performance of CNPs nanofluid was tested by spontaneous imbibition tests. Moreover, the potential EOR mechanism of CNPs nanofluid was discussed and explained by migration mechanism of CNPs nanofluid in pore throats, interfacial activity, and structure disjoining pressure.

## 2. Experimental section

### 2.1. Materials

Petroleum coke and petroleum pitch were obtained from China National Offshore Oil Corporation. Ammonia water and deuterioxide were obtained from Sinopharm Chemical Reagent Co., Ltd. Chemicals including dichloromethane, Tween-80 and sodium chloride (NaCl) were purchased from China Chemical Reagent Co., Ltd. Crude oil was obtained from Xinjiang Oilfield. The mixture of crude oil and kerosene with a density of 0.82 g/cm<sup>3</sup> was used as the oil phase. NaCl solution (3 wt%) with a density of 1.12 g/cm<sup>3</sup> was used as the reservoir saline. The artificial sandstone cores (10 cm in length and 2.5 cm in diameter) were purchased from Haian Oil Scientific Research Instruments Co., Ltd.

### 2.2. Preparation of carbon nanofluid

The preparation process of CNPs nanofluid was shown in Fig. 1. CNPs were prepared according to the reference reported before [36]. We obtained a dark yellow CNPs solution and CNPs powders can be collected after freeze drying. CNPs powders and Tween-80 in a mass ratio of 3:1 were dispersed into water and stirred for 5–10 min to obtain uniformly dispersed carbon-based nanofluid.

### 2.3. Characterization

The morphology of CNPs was detected by JEM-2100 transmission electron microscopy (TEM) of JEOL. The particle size of CNPs nanofluid at different salinities and different temperatures was measured to evaluate the stability of nanofluid. Dynamic light scattering (DLS) and Zeta

potential measurements were conducted by NanoBrook Omni laser particle size analyzer of Brookhaven Instruments Corporation. The interfacial tension was measured using Tracker Automatic Tensiometer produced by TECLIS Interface Technology Co., Ltd. Contact angle was measured using JC2000D2 contact angle measurement of Zhongchen Digital Technic Apparatus Corporation. The residual oil distribution images and  $T_2$  spectrograms of the tight sandstone core during spontaneous imbibition were obtained using a large aperture NMR imaging analyzer from Suzhou NIUMAG Analytical Instruments Corporation. The magnetic field intensity was  $0.3 \pm 0.05$  T, the instrument main frequency was 12.8 MHz, and the probe coil diameter was 150 mm.

### 2.4. Spontaneous imbibition tests and <sup>1</sup>HNMR measurements

Spontaneous imbibition tests were carried out with saturated tight cores. The core parameters are shown in Table 1. Before the tests, the cores numbered 1–5 were saturated with simulated oil and the core numbered 6 was saturated with kerosene. The weight of saturated simulated oil or kerosene in the core was recorded as  $W_1$ . In the tests, the cores were immersed in a permeation bottle filled with different liquids (3 wt% NaCl solution, 0.05 wt% Tween-80 solution, 0.015 wt% CNPs nanofluid, 0.03 wt% CNPs nanofluid and 0.15 wt% CNPs nanofluid), respectively. The bottles were placed in a constant temperature water bath at 75 °C. Spontaneous imbibition tests lasted for 12 days. At the end of the tests, the volume of the collected simulated oil was recorded and converted into weight by density as  $W_2$ . The oil recovery was calculated as follows:

$$\text{Recovery}(\%) = \frac{W_2}{W_1} \times 100\% \quad (1)$$

The migration mechanism of oil droplets in tight core saturated with kerosene during spontaneous imbibition was studied by <sup>1</sup>HNMR measurements. The change of signal strength of proton (H) in kerosene was monitored by <sup>1</sup>HNMR measurements. In this study, D<sub>2</sub>O was used as water phase and kerosene was used as oil phase. The temperature was also set at 75 °C and the spontaneous imbibition test lasted for 12 days. The core was taken out every 4 days during the spontaneous imbibition, and the <sup>1</sup>HNMR spectra and <sup>1</sup>HNMR imaging were measured. The liquid was removed from the surface of the core by using cotton yarn and then the core was wrapped by a preservative film to prevent the volatilization of kerosene. Then,  $T_2$  spectra of <sup>1</sup>HNMR and <sup>1</sup>HNMR imaging at selected times during the spontaneous imbibition were measured.

## 3. Results and discussion

### 3.1. Characterization of CNPs

The TEM image of CNPs was shown in Fig. 2. There was no obvious agglomeration and the particle size was mainly distributed at about 5–10 nm. Through the characterization of DLS, the particle size distribution was shown in Fig. 3. The hydraulic radius of CNPs was about 7 nm, according well with TEM results. The zeta potential value of CNPs was –22.50 mV. The results indicated that CNPs nanofluid was well dispersed and the particle size was small, endowing the nanofluid with flowing in porous media.

### 3.2. Stability of CNPs nanofluid

To study the stability of CNPs nanofluid, the effects of salinity and temperature were clarified. The nanofluid with different concentrations of NaCl from 1 wt% to 18 wt% were prepared. The effect of salinity on particle size of CNPs nanofluid was shown in Fig. 3(a). With the increase of salinities, the average particle size of CNPs nanofluid gradually increased. When the concentration of NaCl solution was <15 wt%,



Fig. 1. The preparation process of CNPs nanofluid.

**Table 1**  
The core parameters.

Number	Length/cm	Diameter/cm	Permeability/mD	Porosity/%
1	3.24	2.52	0.112	13.54
2	3.32	2.51	0.116	13.82
3	3.35	2.50	0.121	13.13
4	3.28	2.51	0.125	13.88
5	3.33	2.51	0.117	13.67
6	2.51	2.50	0.113	13.35

nanofluid still remained clear. The particle size of CNPs nanofluid is always  $<100$  nm until the NaCl concentration reaches 13 wt%, indicating the good stability of CNPs nanofluid at high salinity.

The effect of temperature on particle size of CNPs nanofluid was further investigated. CNPs nanofluid was respectively put into water bath at 30 °C, 40 °C, 50 °C, 60 °C, 70 °C, 80 °C and 90 °C. The particle size of CNPs nanofluid under different temperatures was shown in Fig. 3(b). With the increase of temperatures, the particle size of CNPs nanofluid is always smaller than 10 nm and changes little, indicating that CNPs nanofluid has good stability at high temperature.

### 3.3. Wettability alteration

To investigate the effect of CNPs nanofluid on wettability, the oil-wet glass slides treated with paraffin were aging at three different solutions (3 wt% NaCl solution, 0.05 wt% Tween-80 solution and 0.15 wt% CNPs nanofluid) for 24 h. The contact angles between oil droplets and the glass slides were shown in Fig. 4. The contact angles were about 50° and 75° after immersed in brine and Tween-80 solution, respectively. After treated with brine and Tween-80 solution, the glass slides were still oil-wet. While after immersed in 0.15 wt% CNPs nanofluid, the contact angle was 89°, indicating that the wettability of glass slide changed from oil-wet to neutral-wet. This means that CNPs nanofluid has the stronger ability to change surface wettability than Tween-80 solution and NaCl solution due to the synergistic effect of CNPs and Tween-80. By comparison, the CNPs nanofluid exhibits more excellent capability of surface wettability alteration.

### 3.4. Spontaneous imbibition

The spontaneous imbibition oil recovery with time was shown in Fig. 5. From the curves, all the imbibition oil recovery curves versus

time with different concentrations of CNPs were similar. The imbibition oil recovery gradually increased with the time at the beginning of imbibition process. After about 140 h, the oil recovery almost reached the maximum and kept stable with the time. Through comparison, the oil

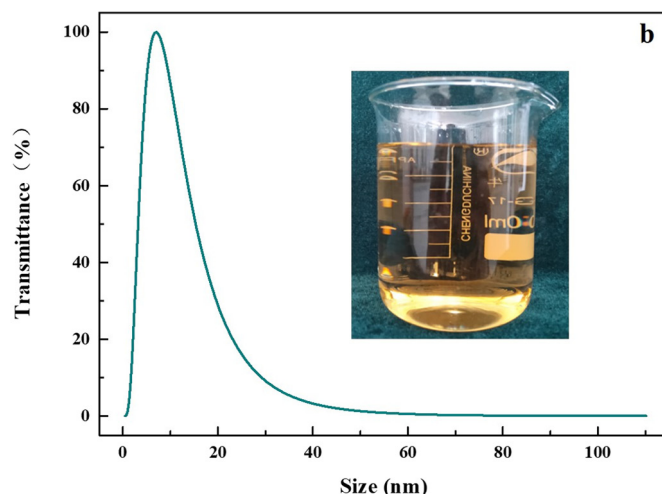
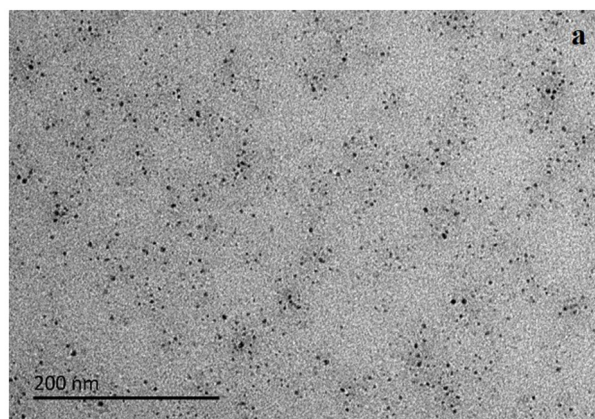


Fig. 2. TEM image(a) and DLS(b) of CNPs.

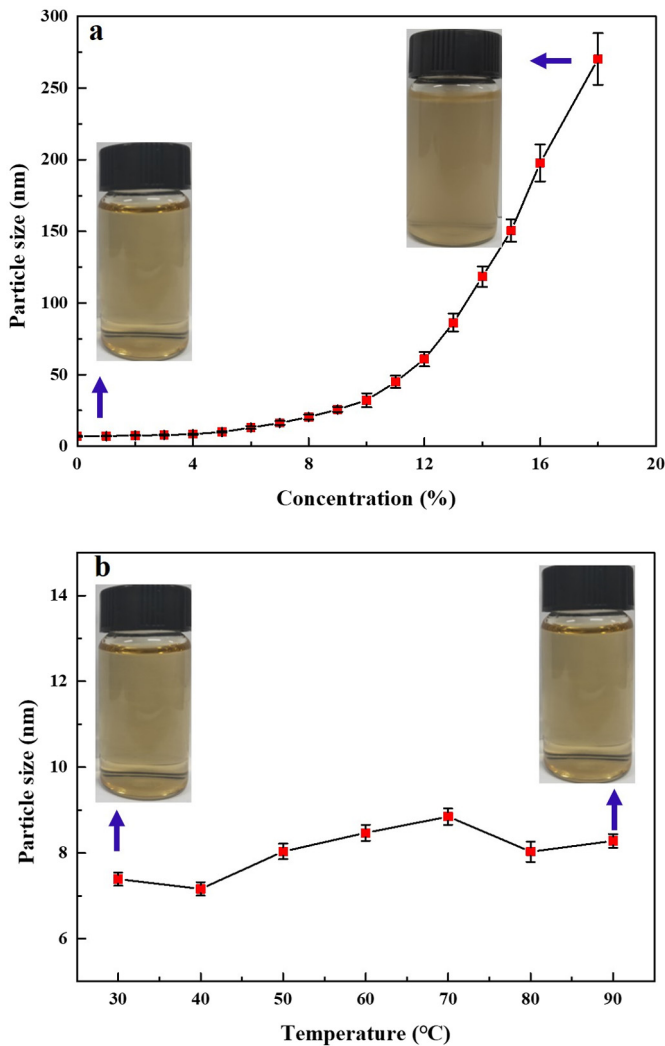


Fig. 3. The particle size of CNPs nanofluid at different salinities(a) and different temperatures (b) error bar = RSD ( $n = 5$ ).

recovery of 0.15 wt% CNPs nanofluid was up to 24%, while the oil recovery of 3 wt% NaCl solution and 0.05 wt% Tween-80 solution was respectively 11% and 16%. CNPs nanofluid performs much higher oil displacement potential than NaCl solution and single Tween-80 solution. Taking 0.15 wt% CNPs nanofluid as an example, the recovery of nanofluid rose rapidly in the first 20 h, and the highest recovery rate could reach 24%. The change tendency of 0.015 wt% and 0.03 wt% CNPs nanofluid was the same as that of 0.15 wt% CNPs nanofluid, while the recovery was lower than that of 0.15 wt% CNPs nanofluid. CNPs nanofluid with higher concentrations has higher oil displacement efficiency. When the CNPs concentration increased from 0.03 wt% to 0.15 wt% by four times, the final imbibition oil recovery was increased <math><2\%</math>. When the concentration reaches a certain extent, increasing the concentration has little significance to enhance oil recovery.

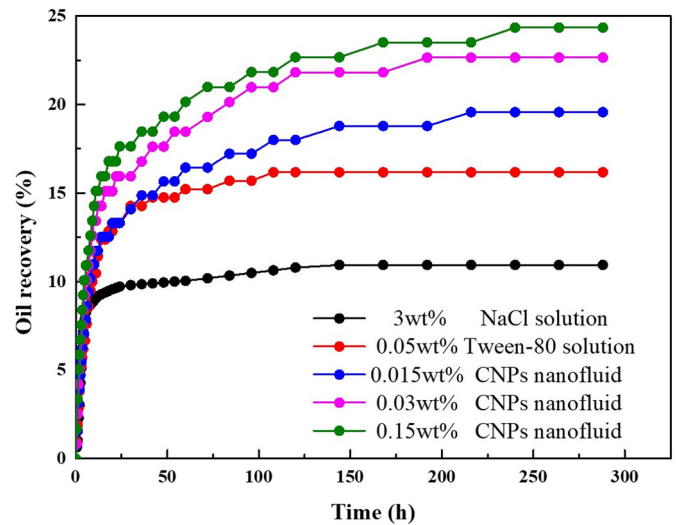


Fig. 5. The oil recovery of 3 wt% NaCl solution, 0.05 wt% Tween-80 solution and CNPs nanofluid of different concentrations.

To further study the spontaneous imbibition process of CNPs nanofluid with the concentration of 0.15 wt%,  $^1\text{H}$ NMR technology was conducted.  $^1\text{H}$ NMR images of the core saturated with kerosene were obtained (Fig. 6). The amount of kerosene and CNPs nanofluid in the core affected the strength of  $^1\text{H}$ NMR signal. The color image showed the change in the amount of kerosene in the core pore throats. In the images, the  $^1\text{H}$ NMR images of the core was more similar to yellow, the signal of kerosene in the core was stronger. And the  $^1\text{H}$ NMR images of the core was more similar to blue, the signal of water phase in the core was stronger. There were a large amount of yellow color part, representing the core pore throats were filled with kerosene and the oil recovery is 0% in this stage. As the spontaneous imbibition process continued, the oil phase signal gradually decreased and the water phase signal gradually increased. This phenomenon suggested that the oil saturation decreased gradually and oil recovery increased. When the spontaneous imbibition continued, the oil phase signal intensities in the middle and edge of cores both decreased and the intensity of the edge decreased more obviously. This phenomenon indicated that the initial oil recovery was due to the oil recovery at the edge of cores, first contacted with the nanofluid. The yellow signal decreased from the edge to the center of core. This was related to kerosene transportation in the pores with the aid of nanofluid. In the early stage of spontaneous imbibition, the oil recovery was constantly increasing and the oil recovery after 4 days can reach 24%. After 8th day, the oil recovery increased by 8% compared with the oil recovery of 4th day. After 12 days, the oil droplets almost stopped flowing and the oil recovery reached the highest value, increased by 2% compared with the recovery of the former 8th day.

### 3.5. Spontaneous imbibition mechanism

To show the detailed migration process of kerosene in pore throats, the  $T_2$  spectra of  $^1\text{H}$ NMR were measured by high-resolution NMR. The

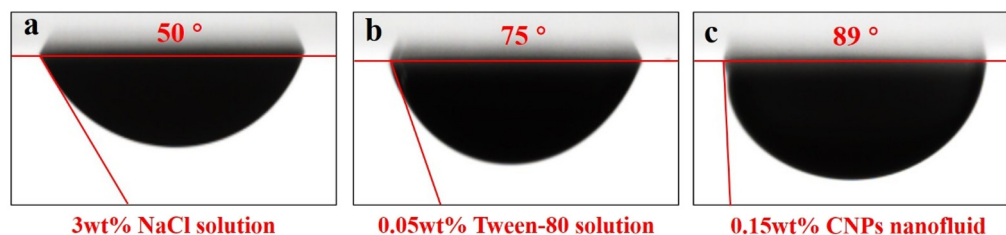


Fig. 4. The contact angles of oil-wet glass slides immersed in different solutions.

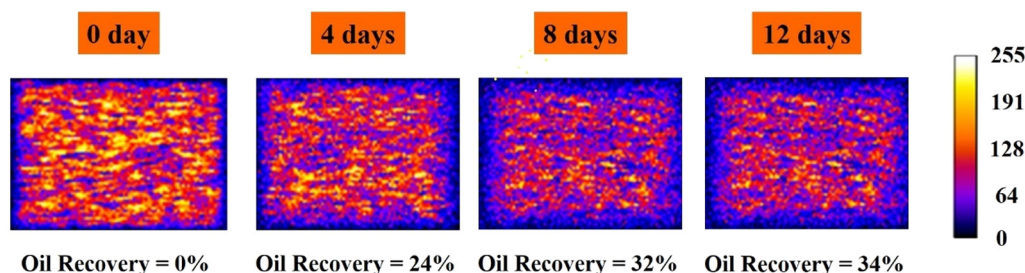


Fig. 6. The imaging analysis of  $^1\text{H}$ NMR in spontaneous imbibition process of tight cores.

results were shown in Fig. 7. The  $T_2$  spectral signals of micropore ( $T_2$  relaxation time  $< 1$  ms) and mesopore ( $1 \text{ ms} < T_2$  relaxation time  $< 100$  ms) decreased obviously in the early stage of spontaneous imbibition, indicating reduction of the oil saturation in cores. The oil in micropores and mesopores were more easily displaced (7.1% and 16.7%, respectively) than that in macropores (0.2%). This was due to the difference of the capillary forces. CNPs nanofluid was imbibed through micropores and mesopores and oil was expelled through macropores. Thus, in the initial stage, micropores and mesopores contributed more to oil recovery. In the middle and later stage of spontaneous imbibition, the change of  $T_2$  spectral signals of macropores was more obvious. The oil in mesopores and macropores is more easily displaced (4.2% and 5.2%, respectively) than that in and micropores (0.6%). Compared with the change of  $T_2$  spectral signal of micropores and mesopores in the initial stage, the change of  $T_2$  spectral signals of macropores in the middle and later stage were not obvious, indicating lower efficiency of oil displacement.

To investigate the effect of CNPs on the interfacial property of oil and water, the interfacial tensions at  $75^\circ\text{C}$  between oil and different fluids were tested. The results were shown in Table 2. Compared with NaCl solution, Tween-80 solution and CNPs nanofluid can obviously reduce the interfacial tension. The interfacial tension of oil/Tween-80 solution was slightly lower than that of oil/CNPs nanofluid. This was due to the adsorption of Tween-80 on the CNPs. CNPs were hydrophilic and they were difficult to adsorb on the surface of oil droplets. After the adsorption of Tween-80 on CNPs, the effective adsorption amount of Tween-80 at the oil/fluid interface will be reduced, resulting to the slightly larger interfacial tension of nanofluid comparing with Tween-80 solution.

To investigate the effect of CNPs on the interfacial wettability of oil and solid, the contact angles with time of different concentrations of

Table 2  
Interfacial tension of oil/fluid.

Fluid	Interfacial tension (mN/m)
3 wt% NaCl solution	27.8
0.05 wt% Tween-80 solution	8.3
0.15 wt% CNPs nanofluid	11.2

CNPs were tested. As shown in Fig. 8, the contact angles of oil/fluid/glass system increased with time. At the initial stage, the contact angles of oil on the oil-wet glass slides were about  $54^\circ$ . After the injection of CNPs nanofluid, the contact angles gradually increased with time. CNPs nanofluid with the concentration of 0.15 wt% changed the contact angle from  $54^\circ$  to  $89^\circ$ . According to the adhesion energy eq. ( $W = \sigma(1 + \cos\theta)$ ), the adsorption of CNPs significantly reduced the adhesion energy required for oil droplets to peel off from pore walls. According to the capillary force equation ( $P_c = 2\sigma \cos\theta/r$ ), capillary force decreases with the increase of contact angles. The oil droplets can pass through the pore throats with little resistance.

According to the experimental results, the spontaneous imbibition mechanism was proposed and shown in Fig. 9. When CNPs nanofluid was seeped into the rock pore throats, CNPs gradually adsorbed on the interface of rock and oil phase. CNPs nanofluid can transform the rock surface from oil-wet to neutral-wet and effectively decrease the interfacial tension based on the interfacial tension tests and contact angle tests. According to the capillary force equation ( $P_c = 2\sigma \cos\theta/r$ ), the capillary force decreases with the decrease of interfacial tensions and the increase of contact angles, making oil droplets flow easily in the pore throats. According to the wedge film theory [36–38], due to the

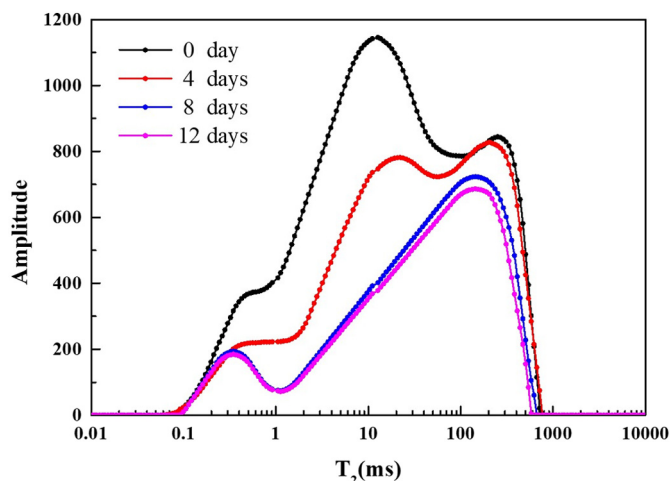


Fig. 7. The  $T_2$  spectra of  $^1\text{H}$ NMR in spontaneous imbibition.

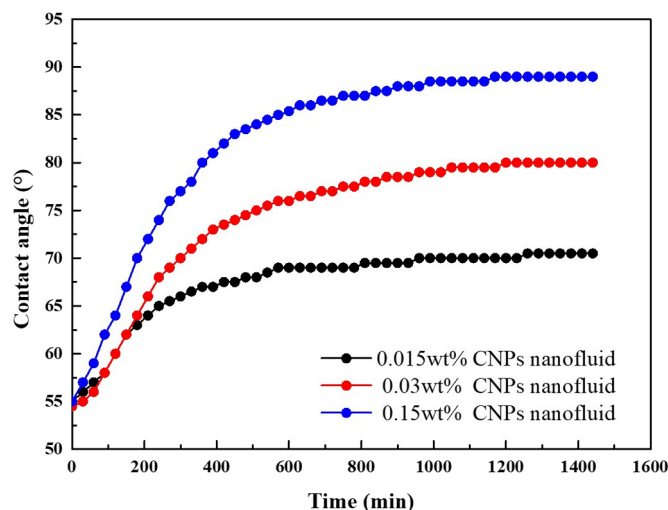


Fig. 8. Dynamic contact angle in different concentrations of CNPs nanofluid.

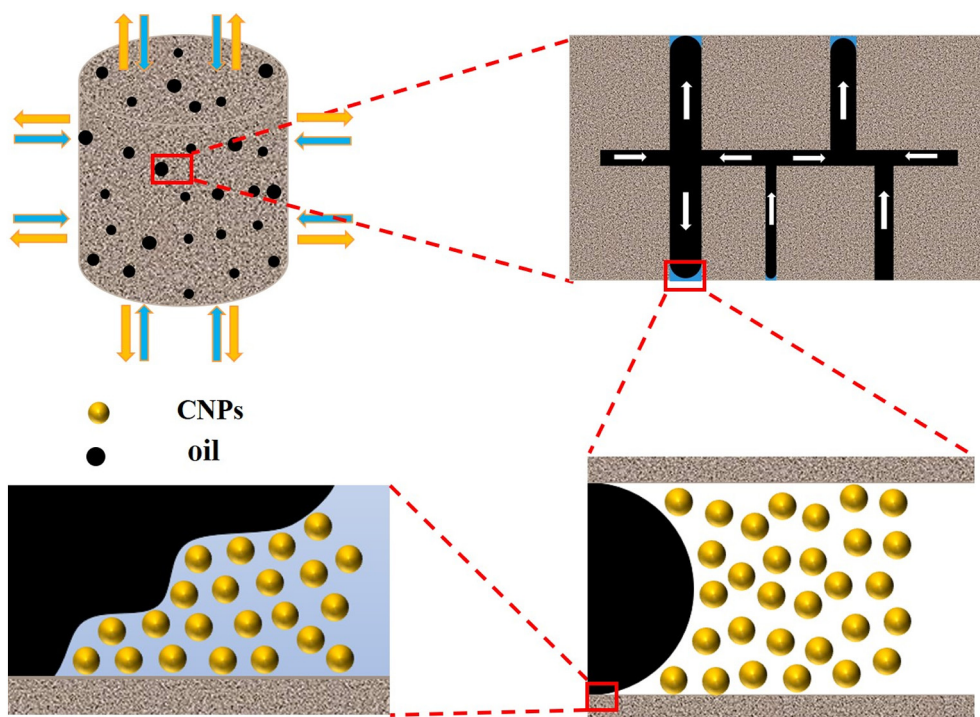


Fig. 9. The image of spontaneous imbibition mechanism.

Brownian motion of nanoparticles and the electrostatic repulsion interactions, when the size of the nanoparticles is small enough and the amount of nanoparticles are much enough, the diffusion force will be generated in the oil/water/solid three-phase contact zone. The diffusion force is unbalanced with the electrostatic repulsion force on the solid surface, and the three-phase contact zone forms a wedge structure. The wedge-shaped structure creates a forward thrust that further spreads the nanofluid in the three-phase contact zone and removes the oil from the pore throats. Under the conditions of interfacial tension decrease, wettability change and structural disjoining pressure, CNPs nanofluid can effectively remove oil droplets adsorbed on the solid surface and discharge them from the pores, thus enhancing oil recovery.

#### 4. Conclusion

In this work, the carbon-based nanofluid was prepared and its dispersion, interfacial activity and spontaneous imbibition were evaluated. 0.15 wt% CNPs nanofluid decreased the interfacial tension to 11.2 mN/m and changed the wettability to neutral wetting. The oil recovery of 0.15 wt% CNPs nanofluid for simulated oil can be up to 24% and that of kerosene can be up to 34%. In addition  $^1\text{H}$ NMR was used to reveal the migration mechanism of CNPs nanofluid in pore throats. Spontaneous imbibition mechanism was concluded by a synergistic effect of the decrease of capillary force and structural disjoining pressure. We expect this work can be useful for the application of carbon nanofluid in tight reservoirs.

#### Notes

The authors declare no competing financial interest.

#### CRediT authorship contribution statement

**Mingwei Zhao:** Writing - original draft, Writing - review & editing. **Xuguang Song:** Writing - original draft, Investigation. **Wenjiao Lv:**

Data curation. **Yining Wu:** Methodology, Validation. **Caili Dai:** Resources, Supervision, Writing - review & editing.

#### Declaration of competing interest

We hereby declare that there is no conflict of interest in this article.

#### Acknowledgments

This work was financially supported by National Natural Science Foundation of China (51874337, 51834010); Natural Science Foundation of Shandong Province (ZR2018QEE003); Changjiang Scholar Program of Chinese Ministry of Education (T2014152); Taishan Scholar Foundation of Shandong Province (tspd20161004) and Fundamental Research Funds for the Central Universities (19CX07001A).

#### References

- [1] H. Chang, B. Liu, J. Crittenden, *Environmental Science & Technology* 53 (2019).
- [2] J.O. Alvarez, D.S. Schechter, *Pet. Explor. Dev.* 43 (2016).
- [3] R.R. Nair, *Journal of Unconventional Oil and Gas Resources* 6 (2014) 1–3.
- [4] C. Jia, M. Zheng, Y. Zhang, *Petroleum Exploration & Development* 39 (2012).
- [5] M. Zhao, H. He, C. Dai, *Energy Fuel* 32 (2018) 2908–2915.
- [6] B. Cai, Y. Ding, H. Shen, *Adv. Mater. Res.* (2014) 962–965.
- [7] Y. Zhou, D. Zhou, *Adv. Mater. Res.* (2015) 1092–1093.
- [8] H. Jia, X. Leng, Q. Wang, Y. Han, *Chemical Engineer Science* 202 (2019) 75–83.
- [9] Y. Zhao, W. Yang, D. Wang, *Small* 14 (2018) 1703216.
- [10] B.Y. Jamaloei, K. Asghari, R. Kharat, *J. Pet. Sci. Eng.* 72 (2010) 251–269.
- [11] A. Mirzaei-Paiaman, M. Masihi, D.C. Standnes, *Transp. Porous Media* 89 (2011) 49–62.
- [12] Y. Meleán, D. Broseta, R. Blossey, *J. Pet. Sci. Eng.* 39 (2003) 327–336.
- [13] M. Zhao, R. Wang, C. Dai, *Chem. Eng. Sci.* 206 (2019) 203–211.
- [14] E.J. Hognesen, D.C. Standnes, T. Austad, *Energy Fuel* 18 (2004) 1665–1675.
- [15] H. Chen, H. Fan, Y. Zhang, *RSC Adv.* 8 (2018) 38196–38203.
- [16] V.C. Santanna, T.N. Castro Dantas, T.A. Borges, *Pet. Sci. Technol.* 32 (2014) 2896–2902.
- [17] D.C. Standnes, *Colloids Surf. A Physicochem. Eng. Asp.* 251 (2004) 93–101.
- [18] B. Wei, Q. Li, F. Jin, H. Li, C. Wang, *Energy Fuel* 30 (2016) 2882–2891.
- [19] Y. Wu, R. Wang, C. Dai, *Industrial & Engineering Chemical Research* 58 (2019) 3707–3713.

- [20] P.S. Hammond, E. Unsal, *Langmuir* 26 (2010) 6206–6221.
- [21] Y. Hurtado, C.C. Beltran, R.D. Zabala, *Energy Fuel* 32 (2018).
- [22] S. Hassanpour, M.R. Malayeri, M. Riazi, *J. Chem. Eng. Data* 63 (2018) 1266–1274.
- [23] M.O. Onyekonwu, N.A. Ogolo, *Society of Petroleum Engineers*, 2010.
- [24] B. Ju, T. Fan, M. Ma, *China Particuology* 4 (2006) 41–46.
- [25] R. Ponnappati, O. Karazincir, E. Dao, *Ind. Eng. Chem. Res.* 50 (2011) 13030–13036.
- [26] L. Hendraningrat, O. Torsaeter, *Appl. Nanosci.* 5 (2015) 181–199.
- [27] M. Zhao, W. Lv, Y. Li, *J. Mol. Liq.* 261 (2018) 373–378.
- [28] C. Dai, X. Wang, Y. Li, *Energy Fuel* 31 (2017) 2663–2668.
- [29] Li Yuyang, Dai Caili, Zhou Hongda, *Energy Fuel* 32 (2018) 287–293.
- [30] O. Zaytseva, G. Neumann, *Chemical and Biological Technologies in Agriculture* 3 (2016) 17.
- [31] Z. Xu, J. Yu, G. Liu, *Sensors Actuators B Chem.* 181 (2013) 209–214.
- [32] C. Wang, S. Lu, *Nanoscale* 7 (2015) 1209–1215.
- [33] H. Soleimania, M.K. Baig, N. Yahya, L. K, *Results in Physics* 9 (2018) 39–48.
- [34] D. Luo, F. Wang, J.Y. Zhu, *Proc. Natl. Acad. Sci. U. S. A.* 113 (2016) 7711–7716.
- [35] Y. Li, C. Dai, H. Zhou, *Ind. Eng. Chem. Res.* 56 (2017) 12464–12470.
- [36] M. Wu, Y. Wang, W. Wu, *Carbon* 78 (2014) 480–489.
- [37] K. Kondiparty, A.D. Nikolov, D. Wasan, K.-L. Liu, *Langmuir* 28 (2012) 14618–14623.
- [38] A. Chengara, A.D. Nikolov, D.T. Wasan, *J. Colloid Interface Sci.* 280 (2004) 192–201.